Spatial Patterning of Thick Poly(2-hydroxyethyl methacrylate) Hydrogels

Stephanie J. Bryant,[†,§] Kip D. Hauch,[†] and Buddy D. Ratner*[,†,‡]

Department of Bioengineering and Department of Chemical Engineering, University of Washington, Seattle, Washington 98195

Received January 20, 2006; Revised Manuscript Received April 8, 2006

ABSTRACT: Patterned hydrogel structures have potential application in microfluidics, tissue engineering, and other soft matter technologies. In this study, we describe a novel photopatterning of *thick* cross-linked poly(2-hydroxyethyl methacrylate) hydrogels through spatial manipulation of polymerization kinetics. Specifically, patterned hydrogels were fabricated by creating an inverse photomask in which the mask allows the initiating light to pass through all areas, but at different intensities. High light intensities, corresponding to the "unwanted regions", cause significant deviations in the polymerization kinetics to result in longer polymerization times compared to lower light intensities. This difference in polymerization kinetics is sufficient to create patterned structures. The novelty of this technique is that monomer molecules are consumed across the solution even in the "unwanted regions", minimizing the adverse effects of diffusion in traditional photolithography. As a result, patterns in relatively thick (∼760 μm) gels can be achieved.

Introduction

Patterned hydrogel structures have potential application in microfluidics,[1−4] tissue engineering,[5−7] and other soft matter technologies. In this study, we describe a novel photopatterning technique that enables patterning of *thick* cross-linked poly(2-hydroxyethyl methacrylate) hydrogels through spatial manipulation of polymerization kinetics.

Hydrogels have been widely used for a variety of biomedical applications due to their biocompatibility and tissue-like physical properties.[8] Specifically, patterned hydrogels have been used to design microfluidic devices with stimuli-responsive channels,[9,10] cell-based microarrays,[11,12] and structures that emulate the complex 3-D tissue environment.[13,14] Recent advances in microfluidic devices for biological applications have turned from the high precision and high cost of silicon-based microelectronic devices to somewhat less precise, lower cost alternatives. Soft lithography is one such alternative approach that utilizes an elastomeric stamp to create 2-D patterns of biological molecules and cells on surfaces as well as 3-D structures such as channels for microfluidics.[15] More recently, patterned hydrogel structures have been fabricated from photopolymerization reactions in combination with a photomask to create 3-D structures. For example, Beebe et al.[1] developed pH-sensitive valves in channels that were patterned into a hydrogel by photopatterning liquid-phase solutions.

For tissue engineering applications, patterned hydrogels can aim to emulate the complex structure of living tissues. Soft lithography has been used to pattern different cell types in 3-D hydrogels to selectively control the microenvironment and spatially control cell position.[16] Photopolymerizations have also been used in combination with a photomask to fabricate multilayers of patterned cells and different cell types for creating a liver equivalent.[6]

Photopatterning has emerged as a simple, inexpensive technique that can be performed in most laboratories to pattern channels for microfluidics[17] or cells in 3-D gels for tissue engineering.[6,13,18] For example, liquid-phase solutions containing monomer, cross-linker, and photoinitiator were polymerized under a photomask to form microfluidic channels in hydrogels that were 250 μm thick with aspect ratios ranging from 4 to 8 (aspect ratio is defined as channel height/channel width).[17] Poly(ethylene glycol) cross-linked gels were photopatterned from liquid-phase solutions to form patterned gels that were 100 μm thick with features that had aspect ratios less than one (aspect ratio is defined and feature height/feature width).[6] Limitations exist with patterning from the liquid phase using photolithography techniques and include low pattern depth and resolution. In general, the thickness of patterned hydrogels has been limited to several hundred microns. Living radical polymerizations have been used to pattern thicker hydrogels (∼300 μm), but these systems require additional components (e.g., photoiniferters) and introduce additional chemistries into the final hydrogel.[10]

Here, we describe a novel and simple technique based on photopolymerization of monomer solutions (containing monomer, cross-linker, and photoinitiator), which enables patterning at greater depths in cross-linked hydrogels through control of the polymerization kinetics.

Photoinitiated free radical polymerization mechanisms are typically comprised of three primary reactions: initiation, propagation, and termination. During initiation, photoinitiator molecules absorb photons of light energy and dissociate into radicals that then react with monomer to form growing kinetic chains (also referred to as macroradicals). The rate of photoinitiation (R_i) is defined by

$$R_i = 2\phi I_a \tag{1}$$

where ϕ is the overall photoinitiator efficiency, I_a is the absorbed light intensity, and the constant 2 derives from the fact that two radicals are formed from each initiator molecule. In samples with appreciable thickness, I_a will vary with sample depth and can be defined by Lambert−Beer's law

$$I_a = I_0(1 - e^{-2.303\epsilon c^* b}) \tag{2}$$

where ϵ is the molar absorptivity of the initiator, c^* is the

[†] Department of Bioengineering.
[‡] Department of Chemical Engineering.
[§] Current affiliation: Department of Chemical and Biological Engineering, University of Colorado, Boulder, CO 80309.
* To whom correspondence should be addressed.

10.1021/ma060145b CCC: $33.50
Published on Web 05/27/2006

instantaneous photoinitiator concentration, and b is the sample thickness. Applying the pseudo-steady-state assumption where the rate of initiation is equal to the rate of termination, the rate of polymerization (R_p) is defined by

$$R_p = k_p[M]\left(\frac{R_i}{2k_t}\right)^{1/2} \quad (3)$$

where k_p is propagation kinetic constant, [M] is the double-bond concentration, and k_t is the termination kinetic constant.

The choice of initiator, initiator concentration, and light intensity are all factors that directly affect the rate of photoinitiation and, subsequently, the rate of polymerization. In general, increases in the rate of initiation will increase the rate of polymerization and ultimately lead to shorter polymerization times required to reach complete conversion of monomer into polymer and a cross-linked hydrogel.[19] Short polymerization times, on the order of seconds, are needed to ensure successful patterning.

During polymerization, the growing length of the polymer chains causes an increase in the viscosity of the reaction mixture. This increase in viscosity leads to a reduction in the mobility of the growing kinetic chains or macroradicals. As a result, these large macroradicals are increasingly unable to diffuse together and terminate. Subsequently, termination becomes diffusion-controlled (i.e., k_t decreases). Small monomer molecules, however, can readily diffuse and propagation continues. As a result, R_p dramatically increases, causing an autoacceleration effect. As the polymerization proceeds toward completion, diffusion of both macroradicals and monomers becomes diffusion-controlled (i.e., k_p and k_t decrease) and R_p drops rapidly, causing an autodeceleration effect. These phenomena are characteristic of chain polymerizations of cross-linked systems.[20]

Results and Discussion

Here, we describe a novel process that takes advantage of the polymerization kinetics to generate patterns in poly(2-hydroxyethyl methacrylate) (poly(HEMA)) hydrogels. The basis for this novel process is that polymerization is initiated across the monomer solution, but at different rates. When the difference is significant, specified regions become cross-linked while other regions are only partially polymerized and remain soluble.

The first step in developing this patterning process was to determine the difference in polymerization kinetics required to achieve a pattern. Photomasks were created using transparency film and a high-resolution printer. Initially, unpatterned masks were produced with a range of opacities from 0 to 100%. The incident light intensity (I_0) was directly proportional to the opacity of the photomasks, where incident refers to the intensity at the top surface of the monomer solution (Figure 1A). Hence, I_0 can be modulated through changes in mask opacity. To determine the effect of mask opacity (i.e., I_0) on the polymerization reaction, double-bond conversion was measured after a 30 s exposure to 365 nm light (Figure 1B). Photomasks with 80−93% opacities (corresponding to I_0's 120−45 mW/cm^2, respectively) resulted in near complete conversion of monomer into a cross-linked hydrogel. As expected, photomasks with opacities greater than 93% opacity (i.e., I_0's below 45 mW/cm^2) resulted in polymerizations with significantly lower conversions after a 30 s exposure. However, unexpectedly, opacities *below* 80% (i.e., I_0's *above* 120 mW/cm^2) also resulted in polymerizations with significantly lower conversions.

The polymerization reaction was also monitored through its completion using two photomasks: one that has high conversion

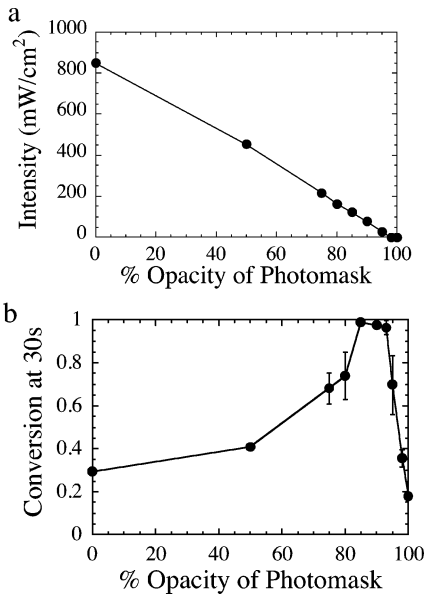

Figure 1. (a) Incident light intensity at 365 nm at the sample surface as a function of the percent opacity of the photomask, where 0% opacity is clear and 100% opacity is black. (b) Conversion of methacrylate photocured for 30 s as a function of photomask opacity.

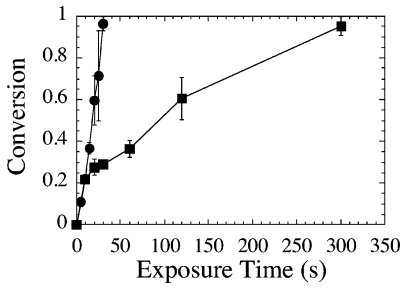

Figure 2. Conversion of methacrylate as a function of polymerization time for samples polymerized under a 93% opacity mask (●) and a 0% opacity mask (■).

(93% opacity) and one that resulted in low conversion, but high I_0 (0% opacity) after a 30 s exposure (Figure 2). Double-bond conversion was similar under both photomasks at low conversions, up to 20%. At longer polymerization times, conversion differed. Under the 93% opacity mask, complete conversion was reached in 30 s, while under the 0% opacity mask, the polymerization reaction occurred at a slower rate, taking 300 s to reach complete conversion. Interestingly, these findings suggest that polymerizations involving high light intensities (120−850 mW/cm^2) deviate from the pseudo-steady-state approximation (eq 3), thus significantly altering the polymerization kinetics and slowing down the overall polymerization time.

Upon irradiation, initiator molecules absorb photons of light energy and dissociate into radicals. A higher I_0 results in a greater number of radicals formed per unit volume per unit time, which leads to a greater number of kinetic chains. As a result, these kinetic chains are shorter.[21,22] Changes in kinetic chain length can have dramatic effects on the polymerization kinetics of cross-linked systems.[22,23] Specifically, a decrease in kinetic chain length causes a decrease in R_p. To examine the length of the kinetic chains during polymerization under the 0 and 93% opacity masks, gel permeation chromatography (GPC) was used. The molecular weights of the kinetic chains were measured after a short exposure time of 10 s where conversion was similar under both photomasks (Figure 2), and the kinetic chains were soluble (i.e., before gelation had occurred). After a 10 s exposure

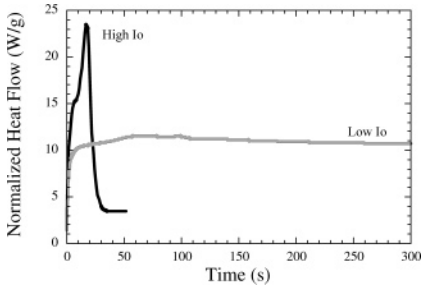

Figure 3. Normalized heat flow as a function of polymerization time for cross-linked poly(HEMA) polymerizations at 40 mW/cm^2 (black line) simulating polymerizations performed with the 93% opacity mask and 720 mW/cm^2 (gray line) simulating polymerizations performed with the 0% opacity masks. Note the polymerized sample absorbs energy from the light source as indicated by constant heat flow postpolymerization and is dependent on the intensity of the light.

under the 0% opacity mask, the average kinetic chain length was 2700 ± 290 Da, while under the 93% opacity mask, the average kinetic chain length was 9200 ± 100 Da. An increase in I_0 from 45 to 850 mW/cm^2 resulted in a 3.4-fold decrease in the average kinetic chain length. To ensure that the high light intensity did not degrade the kinetic chains and subsequently create shorter chains, linear poly(HEMA) was exposed to 365 nm light under the 0 and 93% opacity masks. The average molecular weight of the poly(HEMA) was unaffected by the UV light, indicating that the high I_0 associated with the 0% opacity mask did not cleave the growing chains.

Next, the rate of polymerization was measured for the two systems under the 0 and 93% opacity masks to examine the effects of I_0 and subsequently the differences in the average kinetic chain length on the polymerization reaction. R_p was measured using differential scanning calorimetery (DSC) under isothermal conditions where heat flow measured during the polymerization is directly proportional to R_p. Prior to performing the DSC studies, the reaction temperature was measured by using a thermocouple immersed in the monomer solution. The maximum reaction temperature reached under the 93% opacity mask was 80 °C, while under the 0% opacity mask it was 58 °C. To simulate the reaction conditions of each system under isothermal conditions, the DSC was set to the corresponding reaction temperature. It is important to note that for the low I_0 system a reaction temperature of 80 °C was necessary for the polymerization reaction to reach completion in 30 s (i.e., room temperature required longer polymerization times). The results are shown in Figure 3. Immediately upon illumination, an increase in the rate of polymerization was observed in both samples, signifying the initial conversion of monomer to polymer. As the polymerization proceeds, deviations in the polymerization kinetics are observed under the two initiating schemes. Under the low I_0, the rate of polymerization resulted in polymerization behavior characteristic of cross-linked systems exhibiting distinct autoacceleration and autodeceleration features (i.e., a sharp increase in R_p followed by a sharp decrease in R_p). Under the high I_0, the polymerization behavior had strikingly different features. Most notable are the delayed autoacceleration effect and the significantly lower maximum R_p. Since the growing kinetic chains under the high I_0 are significantly shorter (as determined by GPC), viscosity effects are less pronounced in this system, thus reducing the autoacceleration effect. As a result, longer polymerization times are required to consume monomer. Furthermore, the decreased reaction temperature under the high I_0 further indicates a lower R_p.

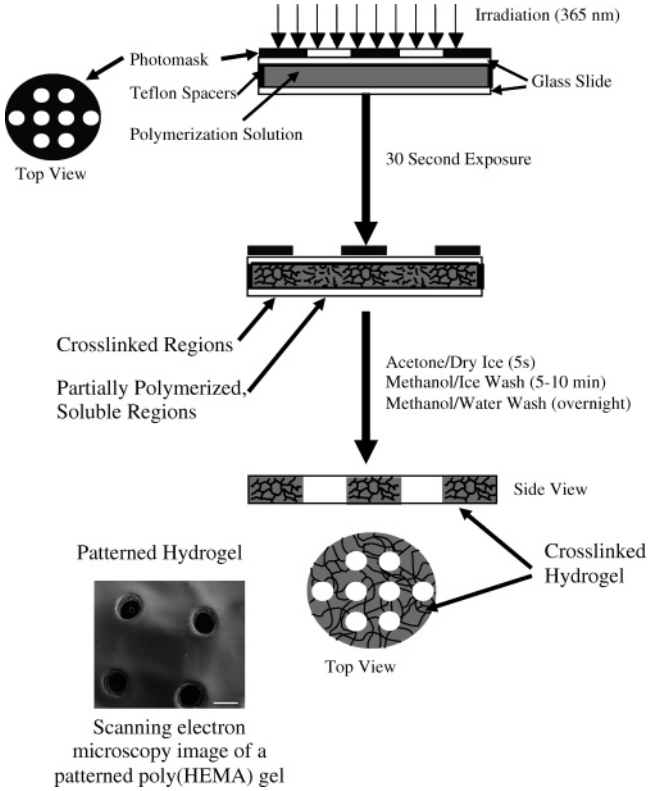

Figure 4. A novel photopatterning technique was developed that is based on differences in polymerization kinetics. This process utilizes a negative photomask, produced on a transparency film, in which the negative pattern of the mask is a shade of gray. The mask is placed on top of the monomer solution configuration (i.e., the monomer solution is placed between two glass slides separated by a Teflon spacer). The sample is irradiated at 365 nm at a light intensity of 4500 mW/cm^2. The photomask enables light transmittance across the mask, but at different intensities depending on the mask opacity. The dark regions absorb a significant amount of the light intensity but enable cross-linking of the gel in 30 s, while the clear regions transmit the high light intensity, resulting in a partially cross-linked, yet soluble region after 30 s. The soluble regions are washed away with a methanol wash. The result is a patterned hydrogel.

On the basis of the differences in polymerization kinetics achieved by using the 0 and 93% opacity masks, we have developed a novel photopatterning process. The process is summarized in Figure 4. A negative photomask was prepared using transparency film and a high resolution printer. A mold consisting of two glass slides separated by Teflon spacers was used with the photomask placed on top. Upon irradiating the sample, the polymerization was initiated across the monomer solution, but at different rates. The regions under the darker mask patterns (i.e., 93% opacity) follow polymerization behavior characteristic of cross-linked systems exhibiting autoacceleration and autodeceleration traits. The polymerizing regions under the clear mask regions (i.e., 0% opacity), however, do not follow the characteristic behavior of cross-linked systems. Under these initiating conditions, the resulting shorter kinetic chains alter the overall polymerization behavior. After 30 s, the polymerization solution under the clear mask regions has not reached the point at which the solution forms a gel (i.e., forms the first cross-link), and the polymer chains remain soluble. Immediately after the 30 s exposure, the partially polymerized, yet soluble polymer was washed away to prevent continued polymerization in the absence of light.[23] Specifically, the mold was dipped in an acetone and dry ice bath for 2 s to reduce the temperature and essentially stop the polymerization reaction followed by a methanol/ice bath for 5−10 min. The gel was removed from

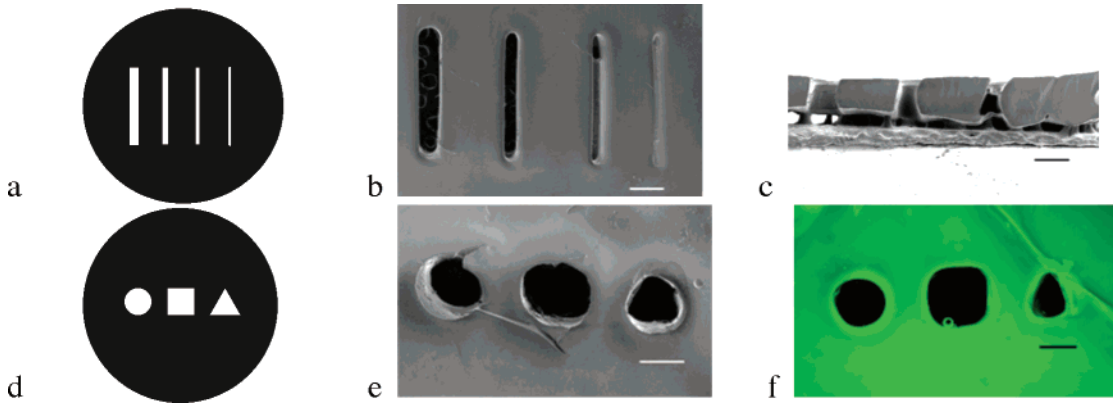

Figure 5. Poly(HEMA) hydrogel structures fabricated from this novel process. The photomask (a, d) shown on the left was used to create the corresponding pattern on the right (b and c and e and f, respectively). The photomask in panel a consists of lines that are 300, 200, 150, and 100 μm in width. Panel c is the cross section of the patterned hydrogel from panel b. Panels b, c, and e are imaged using scanning electron microscopy. The hydrogel patterned structures were also imaged using epi-fluorescence in the hydrated state by adding fluorescein methacrylate to the monomer mixture prior to polymerization (f). The original thickness of the gels was 760 μm, based on the Teflon spacer used in the polymerization setup. The size bar = 500 μm.

the mold and rinsed in a methanol/water (50%/50%) bath overnight to ensure complete removal of the partially polymerized, un-cross-linked poly(HEMA) chains. The resulting patterned hydrogel showed the reverse pattern of the mask. An example of a patterned gel using this novel photopatterning process is shown in the scanning electron micrograph in Figure 4.

A unique attribute of this patterning technique is the fact that monomer molecules are consumed across the sample. This process is unlike traditional photopatterning techniques of liquid-phase solutions, where the unexposed regions contain a high concentration of unreacted monomer—providing a monomer sink into which propagating chains can diffuse and readily react with free monomer, causing polymerization in unwanted regions. For this reason, the depth of patterning is limited in traditional photolithography. Under the scheme presented here, the probability that a propagating chain will encounter a monomer under the high I_0 regions is significantly reduced due to the consumption of monomers across the system. As a result, this process enables patterning at greater depths and consequently thicker patterned hydrogels.

To determine the smallest features achievable with this novel photopatterning technique, a photomask was prepared with line widths of thickness of 100, 150, 200, and 300 μm (Figure 5A). The thickness of the liquid film of monomer solution was 760 μm as dictated by the Teflon spacers used in the mold. The resulting patterned gel is shown in Figure 5B and in cross section in Figure 5C. No pattern was visible under the 100 μm thick line of the mask except for a slight indentation on the surface. However, mask features of 150 μm or greater resulted in a patterned gel. The 150 μm mask feature resulted in bridging. Bridging occurs when the growing kinetic chains in the two regions (low I_0 and high I_0) connect, resulting in a bridge between the cross-linked regions. Evidence of bridging is shown in the cross section of the patterned gel (Figure 5C). Aspect ratios of 4.0 were easily obtainable in gels that were 760 μm thick. The aspect ratio is defined as the channel height divided by channel width. Higher aspect ratios of 5.3 were attainable, but bridging was present. Patterning of thicker hydrogels (1140 μm) was attempted under a 200 μm line width mask. A slight indentation was observed at the exposed side, but no channel was formed (data not shown). Faster removal of the partially polymerized regions (by optimizing the rinse step and/or the mold configuration) may enable higher aspect ratios and thicker gels (>760 μm) to be obtained with this method.

This patterning technique closely reproduced the geometric features of the mask (Figure 5). Various mask features were prepared, and the patterned gel was examined under SEM. The patterned hydrogels were also visualized in the hydrated state by incorporating a small amount of fluorescein methacrylate into the gel. The patterned gels retained the features of the photomask in gels that were 760 μm thick.

In summary, we have developed a novel photopatterning method that is based on spatially controlling polymerization kinetics to develop patterns in *thick* hydrogels. Here, we demonstrated patterning of a poly(HEMA) hydrogel. However, this technique may be expanded to a number of different monomer chemistries where sufficient differences in polymerization kinetics are achieved. We have successfully patterned poly(HEMA) gels with other cross-linkers such as ethylene glycol dimethacrylate and a degradable cross-linker (unpublished results). However, further optimization of this technique is necessary to create smaller features and higher aspect ratios.

This novel patterning technique has the potential to impact a wide range of applications including tissue engineering through the development of novel 3D patterned porous scaffolds (Bryant, Cuy, Hauch, and Ratner, unpublished results), cell biology through the fabrication of patterned hydrogels that mimic natural tissue structures to study cell behavior in 3D, and microfluidics where deep channels are desired.

Experimental Details

Hydrogel Formation. 2-Hydroxyethyl methacrylate (HEMA, Polysciences, Inc.), tetraethylene glycol dimethacrylate (TEGDMA, Polysciences, Inc.), and 2,2-dimethoxy-2-phenylacetophenone (DMPA, Ciba-Geigy) were used as received. The monomer solution was prepared with 2 mL of HEMA as the monomer (80% (v/v)), 92 μL of TEGDMA as the cross-linker (2 mol %, mol of TEGDMA/mol of HEMA), and 37.5 μg of DMPA as the photoinitiator (1.5% (w/w)) in 175 μL of ethylene glycol (Fisher Scientific, Inc.) and 233 μL of distilled water. The monomer solution was purged with nitrogen for several minutes. The polymerization configuration comprised monomer solution placed in a Teflon mold (7 mm diameter punched hole, 760 μm thick) that was sandwiched between two glass slides held together with binder clips. Prior to placing the monomer solution in the Teflon mold, the glass slides were pretreated with glycerol to facilitate removal of the gel. A photomask was designed and printed onto a transparency film using a high-resolution printer (3600 dpi). The photomask was placed on top of the glass slide. This configuration was placed 1 cm below a light guide equipped with a collimating lens adaptor that was

connected to a UV light source (Novacure model 2100, Exfo, Inc.) containing a 365 nm band-pass filter (actual wavelength 335−380 nm). The light intensity was set at 4500 mW/cm^2. Light attenuation due to the 1 cm distance (70% attenuation as per the manufacturer), the blank transparency film (30% absorbance based on UV spectroscopy at 365 nm), and the glass slide (10% absorbance based on UV spectroscopy at 365 nm) resulted in an incident light intensity of 850 mW/cm^2. Immediately after polymerization, the configuration was dipped in an acetone/dry ice bath for 2 s and then placed in a methanol/ice bath for several minutes while the cross-linked gel was removed from the configuration. The gel was then rinsed in a 50% methanol/50% water bath overnight to ensure complete removal of un-cross-linked polymer.

Polymerization Characterization. UV/vis spectroscopy (Hitachi, U-2000) was used to measure the transmittance of light as a function of photomask opacity. Near-infrared (NIR) spectroscopy (Bruker Vector) was used to quantify conversion by monitoring the peak associated with the vinyl group on the monomer and the formation of cross-links after exposure to light. Conversion was calculated by subtracting the ratio of the vinyl peak area (6100−6300 cm^{-1}) of the polymerized sample to the initial vinyl peak area of the sample prior to exposure to light ($n = 3$). The reaction temperature was measured by immersing a thermocouple in the monomer solution during polymerization using the configuration described above with Teflon mold and glass slides. Measurements were taken at 5 s intervals. The rate of polymerization was monitored using differential scanning calorimetry (DSC, Perkin-Elmer DSC-7) under isothermal conditions. The DSC head was removed, and a glass slide was placed over the sample pans to enable transmission of the initiating light to the sample pan. The modified configuration enabled the instrument to maintain a constant temperature during the experiment. The light guide was placed over the sample pan. Light intensity was measured by placing carbon disks (5 mm in diameter) in the sample and reference pans and exposing the disk in the sample pan to the light source and measuring the difference in heat flow. The light intensity was tuned to match the light intensities associated with the 0% opacity mask at 720 mW/cm^2 (higher intensities were not obtainable) and 93% opacity masks at 40 mW/cm^2. In the described configuration, heat flow is associated with heat due to the light source and the polymerization reaction. Heat flow measured from the light was measured in the presence of empty sample and reference pans. Heat flow reached a constant value in 5−7 s after turning on the light source. Approximately 3 mg of monomer solution was placed in the sample pan. Quartz disks were placed over the monomer solution to prevent evaporation. The sample was allowed to equilibrate for several minutes prior to turning on the light source. Heat flow associated with the light source was subtracted from the heat flow associated with the polymerization reaction.

Gel permeation chromatography (GPCmax VE2001, Viscotec equipped with a RI detector 3580) was used to determine the molecular weights of the growing kinetic chains during polymerization. Samples were run in dimethylformamide with 1 wt % LiBr at a flow rate of 1 mL/min at 35 °C and compared against linear poly(methyl methacrylate) standards. The columns used were Tosoh Bioscience alpha-3000 and alpha-4000.

Hydrogel Characterization. Patterned hydrogels were dried under high vacuum overnight. The dried patterned gels were visualized using scanning electron microscopy (FEI Sirion 30, 1 kV beam). To visualize the patterned gels in the hydrated state, fluorescein-*O*-methacrylate (Aldrich) was added to the monomer solution at a final concentration of 0.1% (w/w). Hydrated patterned gels were visualized under light microscopy (Nikon TE200 Inverted microscope equipped with epi-fluorescence).

Acknowledgment. The authors are grateful for the financial support of this research through grants from NIH (R24 HL64387) and a NIH NRSA fellowship (1 F32 HL 74619-01) to S.J.B. Scanning electron microscopy was possible by the NSF supported NanoTech User Facility. Light microscopy was possible through the University of Washington's Engineered Biomaterials NSF-Engineering Research Center program (EEC-95-29161).

References and Notes

(1) Beebe, D. J.; Moore, J. S.; Bauer, J. M.; Yu, Q.; Liu, R. H.; Devadoss, C.; Jo, B. H. *Nature (London)* **2000**, *404*, 588−591.
(2) Hatch, A.; Garcia, E.; Yager, P. *Proc. IEEE* **2004**, *92*, 126−139.
(3) Hutchison, J. B.; Haraldsson, K. T.; Good, B. T.; Sebra, R. P.; Luo, N.; Anseth, K. S.; Bowman, C. N. *Lab Chip* **2004**, *4*, 658−662.
(4) Koh, W. G.; Pishko, M. *Sens. Actuators B: Chem.* **2005**, *106*, 335−342.
(5) Tan, W.; Desai, T. A. *Biomed. Microdevices* **2003**, *5*, 235−244.
(6) Liu, V. A.; Bhatia, S. N. *Biomed. Microdevices* **2002**, *4*, 257−266.
(7) Dhariwala, B.; Hunt, E.; Boland, T. *Tissue Eng.* **2004**, *10* (9/10).
(8) Dumanian, G. A.; Dascombe, W.; Hong, C.; Labadie, K.; Garrett, K.; Sawhney, A. S.; Pathak, C. P.; Hubbell, J. A.; Johnson, P. C. *Plast. Reconstr. Surg.* **1995**, *95*, 901−907.
(9) Beebe, D. J.; Mensing, G. A.; Walker, G. M. *Annu. Rev. Biomed. Eng.* **2002**, *4*, 261−286.
(10) Luo, N.; Metters, A. T.; Hutchison, J. B.; Bowman, C. N.; Anseth, K. S. *Macromolecules* **2003**, *36*, 6739−6745.
(11) Koh, W. G.; Itle, L. J.; Pishko, M. V. *Anal. Chem.* **2003**, *75*, 5783−5789.
(12) Albrecht, D. R.; Tsang, V. L.; Sah, R. L.; Bhatia, S. N. *Lab Chip* **2005**, *5*, 111−118.
(13) Snyder, J. D.; Desai, T. A. *J. Biomater. Sci., Polym. Ed.* **2001**, *12*, 921−932.
(14) Zguris, J. C.; Itle, L. J.; Koh, W. G.; Pishko, M. V. *Langmuir* **2005**, *21*, 4168−4174.
(15) Whitesides, G. M.; Ostuni, E.; Takayama, S.; Jiang, X. Y.; Ingber, D. E. *Annu. Rev. Biomed. Eng.* **2001**, *3*, 335−373.
(16) Tan, W.; Desai, T. A. *Tissue Eng.* **2003**, *9*, 255−267.
(17) Khoury, C.; Mensing, G. A.; Beebe, D. J. *Lab Chip* **2002**, *2*, 50−55.
(18) Koh, W. G.; Revzin, A.; Pishko, M. V. *Langmuir* **2002**, *18*, 2459−2462.
(19) Lovell, L. G.; Newman, S. M.; Bowman, C. N. *J. Dent. Res.* **1999**, *78*, 1469−1476.
(20) Goodner, M. D.; Lee, H. R.; Bowman, C. N. *Ind. Eng. Chem. Res.* **1997**, *36*, 1247−1252.
(21) Burdick, J. A.; Lovestead, T. M.; Anseth, K. S. *Biomacromolecules* **2003**, *4*, 149−156.
(22) Berchtold, K. A.; Lovell, L. G.; Nie, J.; Hacioglu, B.; Bowman, C. N. *Polymer* **2001**, *42*, 4925−4929.
(23) Hacioglu, B.; Berchtold, K. A.; Lovell, L. G.; Nie, J.; Bowman, C. N. *Biomaterials* **2002**, *23*, 4057−4064.

MA060145B